Cross Sections of Elastic Electron and Positron Scattering from Proton-Rich Nuclei

2006 Chinese Phys. Lett. 23 2695

(http://iopscience.iop.org/0256-307X/23/10/020)

Cross Sections of Elastic Electron and Positron Scattering from Proton-Rich Nuclei *

MA Er-Jun(马二俊)[1,2,3], MA Yu-Gang(马余刚)[1**], CHEN Jin-Gen(陈金根)[1], CAI Xiang-Zhou(蔡翔舟)[1], FANG De-Qing(方德清)[1], GUO Wei(郭威)[1,3], LIU Gui-Hua(刘桂华)[1,3], MA Chun-Wang(马春旺)[1,3], SHEN Wen-Qing(沈文庆)[1], SHI Yu(石钰)[1,3], SU Qian-Min(苏前敏)[1,3], TIAN Wen-Dong(田文栋)[1], WANG Hong-Wei(王宏伟)[1], WANG Kun(王鲲)[1], YAN Ting-Zhi(颜廷志)[1,3]

[1]*Shanghai Institute of Applied Physics, Chinese Academy of Sciences, PO Box 800-204, Shanghai 201800*
[2]*Changshu Institute of Technology, Changshu 215500*
[3]*Graduate School of Chinese Academy of Sciences, Beijing 100039*

(Received 26 June 2006)

We investigate the cross sections of the elastic electron or positron scattering from ^{208}Pb, ^{12}C, $^{12,16}O$ and $^{28,32}S$ by the relativistic partial-wave expansion method using the static charge density distribution from the self-consistent relativistic mean field model and also calculate the charge form factor for $^{12,16}O$ and $^{28,32}S$. The numerical results are compared with the available data. Calculations indicate that the extended charge density distributions of ^{12}O and ^{28}S have observable effects on the cross sections of the electron or positron scattering as well as the charge form factors.

PACS: 25. 30. Bf, 21. 10. Ft, 27. 30. +t, 13. 40. Gp

The use of radioactive nuclear beams (RNBs) has led to the discovery of neutron halo nuclei.[1] Theoretically, many calculations have been carried out to predict that there may be proton halos in ^{27,29}S, ^{26,27,28}P,[2] ^{23}Al, and ^{13}N,[3] etc. Although some experimentally measured data indicate some evidence of the existence of proton halos or proton skins in these nuclei,[4] further experiments are needed to confirm their existence. Technical proposals for an electron-heavy-ion collider has been incorporated in the GSI/Germany physics programme[5] as well as the RIKEN/Japan facility.[6] In both the cases the main purpose is to study the structure of nuclei far from the stability line. Since the experimental data for the electron scattering off unstable nuclei will be available soon, it is of interesting to perform an exploratory investigation of elastic electron scattering from proton-rich nuclei.

There are some methods that can be used to calculate the differential cross sections for the elastic high-energy electron scattering off nuclei. The conventional methods are the distorted wave Born approximation,[7] the relativistic eikonal approximation[8] and the relativistic partial-wave expansion method.[9] The partial-wave expansion method can used to deal with both electron and positron elastic scattering off nuclei, so we utilize it to obtain the differential cross sections for electron or positron scattering off the exotic nuclei.

Some theoretical models can give reliable charge density distribution for stable nuclei. The typical models include the Skyrme–Hartree–Fork model,[10] the ab initio no-core shell model,[11] the large-scale shell model method[12] and the self-consistent relativistic mean field (RMF) model. A series of calculations[13−16] have shown that the RMF model can reproduce the binding energies, the separation energies and the radii of nuclear charge density distribution, with good precision. Therefore we use the RMF model to calculate the nuclear ground-state charge distribution.

The core of the relativistic partial expansion method is to solve a Dirac equation for the electron or positron. We assume that the charge distribution of the target nucleus is spherically symmetric. The electrostatic interaction energy between the projectile and the target nucleus reads

$$V(r) = Z_0 e\varphi(r), \tag{1}$$

where $Z_0 e$ is the charge of the projectile ($Z_0 = -1$ for electron and $+1$ for positron) and $\varphi(r)$ is the electrostatic potential of the target nucleus. Let $\rho_{ch}(r)$ denotes the charge density of the target nucleus, we have

$$\varphi(r) = e\Big(\frac{1}{r}\int_0^r \rho_{ch}(r')4\pi r'^2 dr' + \int_r^\infty \rho_{ch}(r')4\pi r' dr'\Big). \tag{2}$$

The scattering of relativistic electrons or positrons by a central field $V(r)$ is completely described by the direct scattering amplitude $f(\theta)$ and the spin-flip

* Supported partially by the Shanghai Development Foundation from Science and Technology under Grant Nos 05XD14021 and 06QA14062, the National Natural Science Foundation of China under Grant No 10328259, 10135030 and 10535010, and the Major State Basic Research and Development Programme under Grant No G200077404.

** To whom correspondence should be addressed. Email: ygma@sinap.ac.cn

scattering amplitude $g(\theta)$.[17] The elastic differential cross section in the relativistic partial-wave expansion method can be expressed as

$$\frac{d\sigma}{d\Omega} = |f(\theta)|^2 + |g(\theta)|^2. \quad (3)$$

After the differential cross sections are obtained, we can calculate the charge form factors $F(q)$ by dividing the differential cross sections with the Mott cross section $(d\sigma/d\Omega)_{\rm Mott}$[18]

$$|F(q)|^2 = \frac{d\sigma/d\Omega}{(d\sigma/d\Omega)_{\rm Mott}}. \quad (4)$$

In Fig. 1, we show comparisons of electron and positron elastic scattering cross sections with the experimental data[19] for ^{208}Pb and ^{12}C using a static charge density calculated by the RMF model with the NL-SH parameters. The part of the Coulomb effect associated with the acceleration of the lepton by the Coulomb potential of the nucleus corresponds[20] to the effective momentum transferred between the lepton and the nucleus depending on the sign of the lepton's charge. This shifts the apparent location of the diffraction minima. The effects of the Coulomb distortion and the different effective momentum transfer are clearly visible in Fig. 1(a). The locations of the diffraction minima are shifted between electrons and positrons due to the change in the effective momentum transfer, and the magnitudes of the cross sections at the same effective momentum transfer differ due to differences in the Coulomb distortion. Clearly, an electron–positron comparison is highly sensitive to the Coulomb distortion effects, and the calculation is generally in agreement with the measured data. Figure 1 also displays the theoretical cross sections and their ratios for ^{12}C compared to the experimental data. The good agreement between the experimental results and theoretical calculations for the ^{12}C data is also reached.

For each incident energy and momentum transfer we determine the ratio $R = (d\sigma/\Omega)|_{e^+}/(d\sigma/\Omega)|_{e^-}$ for both the measured data and the theoretical calculation. Figures 1(b) and 1(d) display the theoretical and experimental values of R for ^{208}Pb and ^{12}C. The theoretical ratios are generally in good agreement with the measured ones.[19]

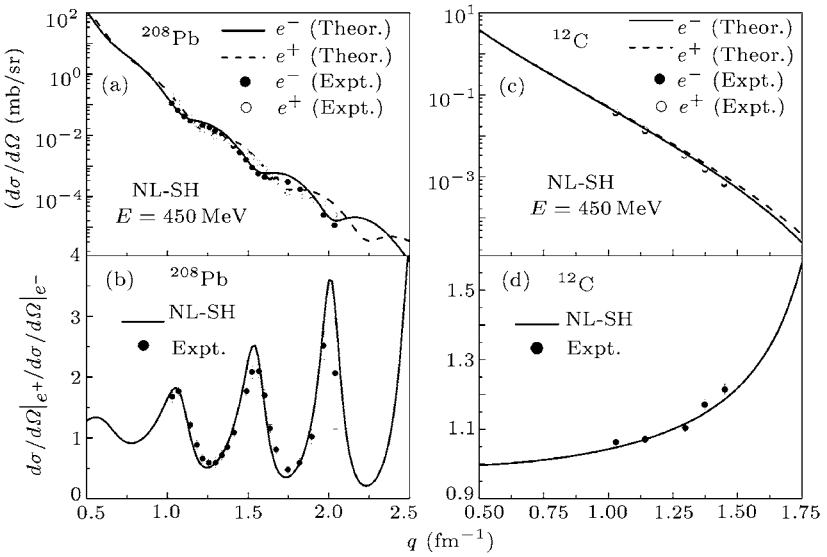

Fig. 1. Positron and electron elastic scattering cross sections and their ratios for ^{208}Pb [(a) and (b)] and ^{12}C [(c) and (d)].

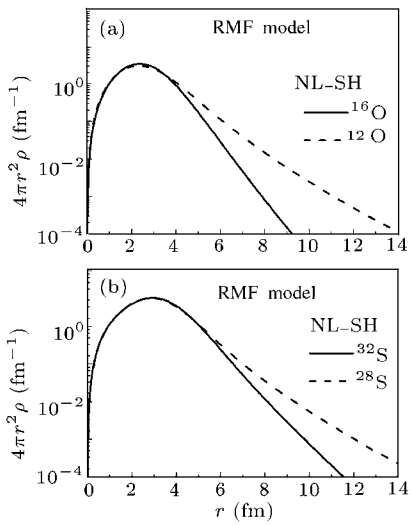

Fig. 2. Charge density distribution of ^{12,16}O and ^{28,32}S calculated with the NL-SH force parameters.

From Fig. 1, it is obvious that the combination of the relativistic partial-wave method with the RMF model can give reasonable cross sections of high-energy electron or positron scattering off nuclei, and the RMF model can produce the ground state charge density distribution of nuclei.

The charge density distributions of ^{12,16}O and ^{28,32}S are displayed in Fig. 2. It can be seen that the charge density distributions of ^{28,32}S with the NL-SH parameters are different although the two nuclei have the same proton number. The weak binding of the last two protons in ^{28}S leads to the extended charge density distribution. This agrees with the theoretical calculations,[2,16] and with the experimental results[4] of the neighbouring nuclei ^{26,27,28}P. A similar conclusion holds true for ^{12,16}O.

Figure 3 displays the positron and electron elastic scattering cross sections and their cross section differences for ^{12}O and ^{16}O at different incident energies. The cross sections of the positron and electron elastic scattering off ^{28,32}S for different incident energies are plotted in Fig. 4. The difference between the cross

sections $D(q)$ in both the figures is defined as

$$D(q) = \frac{(d\sigma/d\Omega)|_{e^-} - (d\sigma/d\Omega)|_{e^+}}{(d\sigma/d\Omega)|_{e^-} + (d\sigma/d\Omega)|_{e^+}} \qquad (5)$$

for electron- and positron-scattering from the identical nucleus. From Figs. 3 and 4, we can deduce the following conclusions.

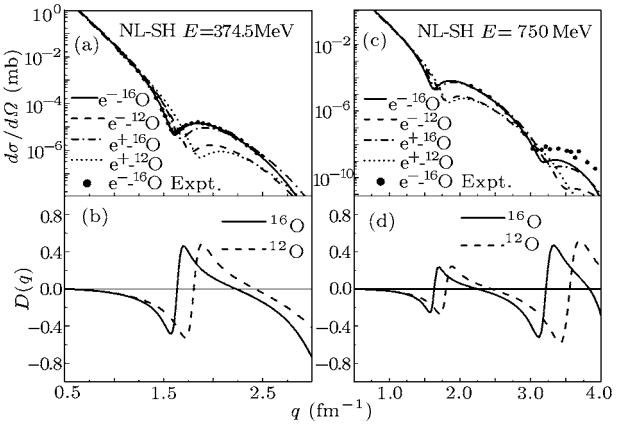

Fig. 3. Positron and electron elastic scattering cross sections and their cross section differences for ^{12,16}O.

Firstly, it is apparent that the calculated cross sections of electron scattering both for ^{16}O and for ^{32}S almost coincide with the experimental data[21,22] in the range of low and moderate momentum transfers ($q \leq 3\,\mathrm{fm}^{-1}$). Theoretical results are in very good agreements with the experimental data in this range of momentum transfers. At high-momentum transfers, a deviation occurs between the theoretical cross sections and the experimental data. Since the cross section in this range of momentum transfers is mainly sensitive to the details of the inner part of the charge density distribution,[21] its occurrence indicates that the theoretical charge density distribution has a departure from the experimental one around the centre of the nucleus. This means that the RMF model can reproduce the charge density distribution for ^{16}O and ^{32}S very well except near the centre of the nucleus. The combination of the relativistic partial-wave method with the RMF model can predict the cross sections of the elastic electron–nucleus scattering from the stable isotopes of O and S.

Secondly, the cross sections of electron scattering for the unstable proton-rich nuclei ^{12}O and ^{28}S display the outward shifts of the positions of the diffraction minima as compared to the stable isotopes ^{16}O and ^{32}S. The differences between the cross sections both for ^{12}O and ^{16}O at the first minima of momentum transfer and for ^{32}S and ^{28}S at the second minima of momentum transfer are large enough to be observable in the experiments. Since the difference of the charge density distributions both for ^{12}O and ^{16}O and for ^{28}S and ^{32}S is mainly caused by the difference of the charge density distributions of the last two protons in ^{12,16}O or ^{28,30}S, the information of the density distribution of the last two protons could be extracted by comparing the cross sections of ^{12,16}O or of ^{28,30}S.

Thirdly, the cross sections of positron scattering from the stable nuclei ^{16}O and ^{32}S have similar trends as compared with the ones of electron scattering from the same nucleus. Like the electron scattering from the unstable nuclei ^{12}O and ^{28}S, the positions of the diffraction minima of the cross sections of positron scattering from the unstable nuclei ^{12}O and ^{28}S shift outward in comparison to the positron scattering from the stable nuclei ^{16}O and ^{32}S. The difference between the cross sections of positron scattering off the stable nucleus and the corresponding unstable isotope is clearly distinguishable in the positron–nucleus scattering experiment. Thus one can presume that the conclusions of analysis of electron–nucleus scattering still hold true for the positron–nucleus scattering, and the measurement and comparison of the cross sections of the positron scattering from unstable nucleus and the corresponding stable nucleus can provide the information of the ground-state charge density distribution of unstable proton-rich nuclei.

Fourthly, from analysis of the variation of the differences of the cross sections $D(q)$ with momentum transfer, one can deduce that the locations of diffraction minima of the cross section for the positron–nucleus scattering are shifted as compared with the electron–nucleus scattering. This shift is due to the different Coulomb effects of the target nucleus on electron and positron. The differences of the cross sections $D(q)$ oscillate irregularly and the amplitudes of $D(q)$ increase with momentum transfer. In the range of low momentum transfers, the solid curve (for ^{16}O and ^{32}S) coincides with the dashed curve (for ^{12}O and ^{28}S). This indicates that the differences of the cross sections between stable nucleus and corresponding unstable isotope can be observed in electron- or positron-scattering experiments only when the momentum transfers are larger than a certain value.

For the purpose of comparing the experimental data of electron–nucleus scattering at different incident energies, we calculate the charge form factor of ^{12,16}O and ^{28,32}S. Figure 5 displays the squared form factors of ^{12,16}O and of ^{28,32}S. The experimental cross sections for ^{16}O and ^{32}S are taken from Refs. [21,22]. It can be seen from Fig. 5 that the location of the first minimum of the form factor of ^{12}O and the position of the second minimum of the form factor of ^{28}S shift outward markedly as compared with ^{16}O and ^{32}S. In addition, the amplitude of the form factor has a significant deviation, especially in the neighbourhood of the two minima. The shifts of the two minima and the amplitude deviation of the form factor are large enough

to be observable. Since the form factor is connected to the charge density distribution by a Fourier transformation, the elastic electron scattering form factor of a nucleus is directly related to its charge density distribution, which is mainly determined by the density distribution of protons in a nucleus. The weak-binding of the last two protons in ^{12}O and ^{32}S leads to the extended charge density distribution, which results in the minimum shifts and the amplitude deviation of the form factors of ^{12}O and ^{28}S as compared with ^{16}O and ^{32}S. These effects should be observable and show that elastic electron–nucleus scattering can be used as an effective tool to study proton drip-line nuclei.

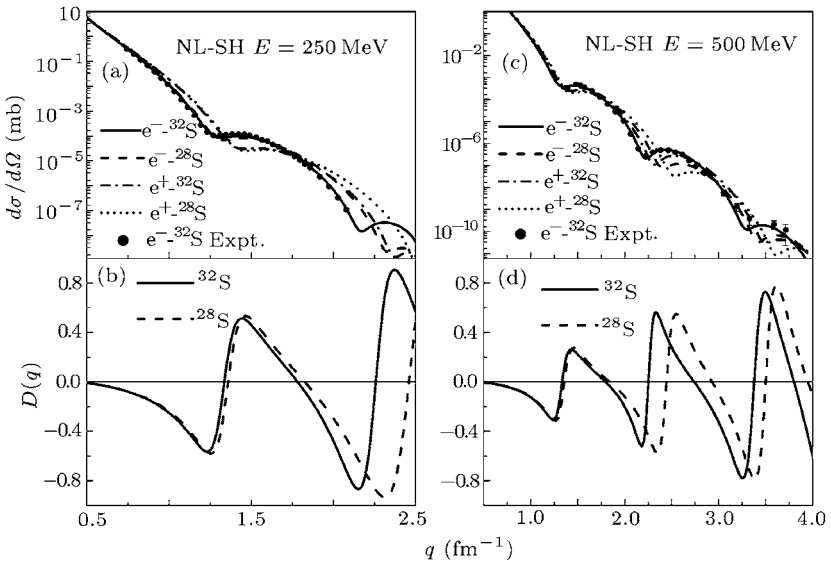

Fig. 4. Positron and electron elastic scattering cross sections and their cross section differences for ^{28,32}S.

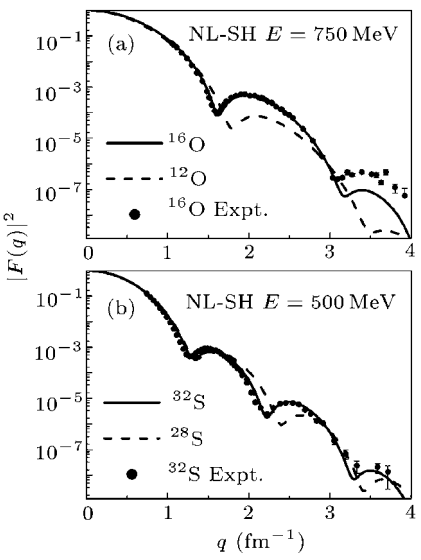

Fig. 5. Squared charge form factor for ^{12,16}O and ^{28,32}S.

In summary, we have combined the RMF model with the relativistic partial-wave expansion method to investigate the elastic electron- or positron–nucleus scattering. Calculations indicate that the present theory is reliable for the elastic electron- or positron–nucleus scattering. In comparison with electron, positron scattering from a nucleus displays the minimum shift and the amplitude deviation of the cross section (in the same momentum transfer), which is due to the different Coulomb effects of a nucleus on positron and electron. As compared to the stable nuclei ^{16}O and ^{32}S, both the shifts of the minimum and the amplitude deviations of the cross section or the form factors of ^{12}O and ^{28}S result from the existence of the long tail of the charge distribution, which is essentially attributed to the influence of the charge density distribution of the last two protons in ^{12}O and ^{28}S. Since the differences of the cross sections and form factors between a stable nucleus and its proton drip-line isotopes are large enough to be experimentally observable, the elastic electron- or positron–nucleus scattering is an effective tool to investigate proton-halo phenomena of proton-rich nuclei.

References

[1] Tanihata I et al 1985 *Phys. Rev. Lett.* **55** 2676
[2] Brown B A et al 1996 *Phys. Lett.* B **381** 391
Ren Z et al 1996 *Phys. Rev.* C **53** R572
[3] Zhang H Y et al 2003 *Nucl. Phys.* A **722** C518
Chen J G et al 2004 *Chin. Phys. Lett.* **21** 2140
[4] Zhang H Y et al 2002 Nucl. Phys. A **707** 303
Cai X Z et al 2002 *Phys. Rev.* C **65** 024610
Liu Z H et al 2004 *Chin. Phys. Lett.* **21** 1711
Wei Y B et al 2005 *Chin. Phys. Lett.* **22** 61
[5] Haik Simon 2005 *Technical Proposal for the Design, Construction, Commissioning, and Operation of the ELISe Setup* (GSI Internal Report, December 2005)
[6] Suda T et al 2001 *Proposal for the RIKEN Beam Factory* (RIKEN, 2001)
[7] Antonov A N et al 2005 *Phys. Rev.* C **72** 044307
[8] Wang Z et al 2004 *Phys. Rev.* C **70** 034303
[9] Yennie D R et al 1954 *Phys. Rev.* **95** 500
[10] Richter W A et al 1954 *Phys. Rev.* C **67** 034317
[11] Hasan M A et al 2004 *Phys. Rev.* C **69** 034332
[12] Karataglidis S et al 1997 *Phys. Rev.* C **55** 2826
[13] Gambhir Y K et al 1990 *Ann. Phys.* (N.Y.) **198** 132
[14] Horowitz C J et al 1981 *Nucl. Phys.* A **368** 503
[15] Ma Z et al 1994 *Phys. Rev.* C **50** 3170
[16] Ren Z et al 1999 *Nucl. Phys.* A **652** 250
[17] Walker D W 1971 *Adv. Phys.* **20** 257
[18] Hofstadter R 1956 *Rev. Mod. Phys.* **28** 214
[19] Breton V et al 1991 *Phys. Rev. Lett.* **66** 572
[20] Yennie D R et al. 1965 *Phys. Rev.* B **137** 882
[21] Sick I et al 1970 *Nucl. Phys.* A **150** 631
[22] Li G C et al 1974 *Phys. Rev.* C **9** 1861